Crystal structure of nickel-reconstituted haemoglobin – A case for permanent T-state haemoglobin

Swarnalatha Venkateshrao[†], S. Deepthi[#], V. Pattabhi[#] and P. T. Manoharan[†,*,§]

[†]Department of Chemistry and Regional Sophisticated Instrumentation Centre, Indian Institute of Technology – Madras, Chennai 600 036, India
[#]Department of Crystallography and Biophysics, University of Madras, Chennai 600 025, India
[§]Jawaharlal Nehru Centre for Advanced Scientific Research, Jakkur, Bangalore 560 064, India

The three-dimensional crystal structure of nickel-reconstituted human haemoglobin (NiHb) is determined by X-ray crystallography at 2.5 Å resolution. The final refined model, when compared with deoxy haemoglobin, clearly reveals a permanent T-state conformation of NiHb. The tertiary changes associated with the alpha subunit are larger in magnitude than those in beta subunits. However, there are some significant quaternary changes observed at the interfacial regions arising out of the perturbations associated with the Ni haeme in the alpha subunit. The central metal ion in the two alpha subunits and one of the beta subunits is clearly four-coordinated, while the other beta subunit reveals a greater tendency for the metal ion to be five-coordinated at the heme site. This result is consistent with the earlier findings like optical, resonance Raman, NMR, and spin-labelled EPR studies on NiHb, which show two different metal ion environments in NiHb, interpreted as due to four and five-coordination. Hence it is clear that there is inequivalence between the two beta subunits in addition to the heterogeneity observed among the alpha and beta subunits. Crystallographic evidence revealing the presence of a five-coordinated nickel(II) porphyrin complex is a special feature of interest presented here.

COOPERATIVE ligand binding in haemoglobin (Hb) has been a subject of immense interest over the past few decades[1–3]. Several theories were put forth in order to explain the origin of such cooperativity[4–8] (MWC model[4], Pauling model[5], KNF model[6], Perutz's 'triggering mechanism'[7] and the Acker's symmetry rules[8]). The stereochemical mechanism proposed by Perutz is based on the X-ray structures of two alternate structures, the deoxyHb designated as the T- (tensed) state and the oxy R- (relaxed) state. In order to understand the molecular mechanism of cooperative ligand binding in heme proteins, it is necessary to investigate in detail the structures of fully unligated and ligated molecules and compare the structural changes with those of the intermediate species associated in the T ↔ R transition. The central metal ion in heme proteins is recognized as the principal site of interaction and hence plays an important role in elucidating the structure–function relationship. The reconstitution experiments in which the central metal atom Fe(II) is replaced by similar transition metals such as Ni(II), Cu(II), Co(II), Mg(II), Mn(II), Zn(II) have proved useful in providing a good deal of information on the electronic and spin states of the metal ion which are responsible for the global conformation of the molecule[9]. The primary approach for a better understanding of the structure–function relationship at the atomic level is obtained from the X-ray structure of the protein species involved. Crystals of reconstituted MgHb[10], MnHb[11], CoHb[12] and hybrid Hbs such as Fe–Co[13], Ni-Fe[14], Fe-Ni[15], Mg-Fe[16], Fe-Mn[17] have been studied by X-ray structure analysis. Spectroscopic, physical and chemical studies on these reconstituted heme proteins have provided certain interesting features over the past few years which have led to a better investigation on the structural and chemical basis of heme–heme interaction.

Metal ions such as Cu(II), Ni(II)[18–20] and Mg(II)[16] have been considered as good reporter groups for stabilizing a T-state conformation of the molecule. In particular, Cu(II) and Ni(II) do not bind either CO or O_2, and hence they are regarded as very stable species representing a permanent deoxy T-state molecule, as also suggested on the basis of chemical reactivity studies using 4,4′-pyridine disulphide (PDS)[19]. Oxygen-binding studies on Ni–Fe hybrids have proved that Ni(II) protoporphyrin IX is a suitable model for a permanent deoxy heme[20]. The most interesting feature in case of NiHb is the presence of two different metal ion sites, a four-coordination and a five-coordination as revealed by earlier spectroscopic studies[18,19,21–23]. The fifth coordination is satisfied by the N(ε) of the proximal histidine of the protein chain, which is unique in case of the nickel porphyrins. We report here a detailed analysis of the crystal structure of NiHb and its comparison with deoxyHb. This work was particularly chosen in order to investigate the similarities and differences between NiHb and deoxyHb, both being T-state

*For correspondence. (e-mail: ptm@rsic.iitm.ernet.in)

molecules. It is also of interest to investigate the presence of two different metal ion sites existing in the same molecule.

Materials and methods

Crystallization, data collection and processing

Human Hb was first separated from RBC, and purified further by well-established methods[24]. Reconstituted Ni(II) Hb was prepared and purified as described earlier[23]. Crystals were grown in batch method from a 15% (w/v) polyethylene glycol-8000 and a 4% Hb solution at room temperature for 10–14 days. The X-ray data were obtained (Table 1) using the Mar Research Image plate system, processed and scaled using Mar XDS at the Molecular Biophysics Unit, Indian Institute of Science, Bangalore. The crystal-to-detector distance was 100 mm. The intensity data were collected for every 1° rotation in the phi axis and the exposure time was maintained at 300 s per frame. A total of 111 frames corresponding to 90° rotation in the phi axis were collected. The crystals diffracted to a resolution of 2.5 Å, and belong to the space group $P2_12_12$ with cell parameters: $a = 95.2$ Å, $b = 96.3$ Å, $c = 65.2$ Å. The data were processed and scaled using MAR XDS.

Structure solution and refinement

The structure was solved by the molecular replacement method using X-PLOR[25], with the partially oxygenated T-state human Hb[26] as the search model. A non-crystallographic symmetry along the psuedo dyad axis was assumed throughout the refinement. A consistent solution at $\Theta_1 = 0$, $\Theta_2 = 0$ and $\Theta_3 = 0$, and a translation at $\delta x = 0$, $\delta y = 0.25$, $\delta z = 0$, appeared in five different resolution ranges. The rigid body refinement led to a R-factor of 0.38 and R-free = 0.41, with a 2σ cut-off at a resolution range of 8.0–2.5 Å. Subsequently, a few cycles of positional refinement resulted in a R-factor of 29% and R-free of 39%. The structure was further refined and the model corrected using $2F_o–F_c$ and $F_o–F_c$ maps employing the program 'O'. Thirty-eight water molecules were located and further refinement gave a R-factor of 24.2% and R-free = 32.4%. The final refinement parameters are listed in Table 2. The final refined coordinates have been deposited in the Brookhaven Data Bank (PDB ID 1FN3).

Table 1. Output summary of X-ray data collection

Minimum and maximum resolution (Å):		19.8, 2.5
Number of observations in input	:	75819
Number of reflections with $i = 0$	:	15810
Number of rejected reflections	:	0
Number of anomalous differences	:	15959
Number of unique reflections in output:		19946
Multiplicity of data set	:	3.8
Completeness of data set	:	91.4%
R-factor on intensities	:	15.5%

Results

Reference frames

To examine the structural differences between deoxyHb and NiHb structures, we have chosen three principle reference frames: (i) Baldwin and Chothia[27] used the $\alpha_1\beta_1$ interface as a reference frame for comparing the T and R states of the molecule. This comprises largely parts of the B, G and H helices of both chains. We have adopted here for α residues B 20–36, G 98–112 and H 118–134; for β residues B 20–33, G 104–116 and H 125–139 as the 'BGH reference frame'. (ii) 'F-helix frame' which illustrates the extent of conformational change at the F-helix, FG-corner and heme. (iii) 'Heme frame' which illustrates the differences in the coordination sphere of the central metal ion.

Comparison of deoxyHb and NiHb structures

When the structure of NiHb is superimposed on deoxyHb[28], the rms difference is found to be 0.8 Å for all main-chain atoms. The rms difference for all the backbone atoms at the $\alpha_1\beta_1$ interface for the two structures is 0.6 Å, suggesting that there is no significant structural difference occurring at this interface.

Tertiary structural changes in the α-subunit

The rms difference for all the main-chain atoms at the BGH reference frame is 0.7 Å for both α_1 and α_2. When the heme groups are superimposed (Figure 1 *a*), significant shifts in E- and F-helices are observed in both the α-subunits. The residue vs rms deviation for the superposition of α_1 chains of NiHb over deoxyHb molecule is shown in Figure 1 *b*, specially to clearly see the shift in the E-helix. The E-helix has moved in a direction perpendicular to the helical axis, and away from the heme. This movement of the E-helix is further continued in such a way that the F-helix is significantly moved out, thereby pulling the proximal histidine away from the heme pocket. Figure 1 *a* indicates a significant shift in the main-chain conformation of the F-helix residues, which is propagated till the beginning of the FG-corner. The rms difference for the main-chain atoms at the FG-corner is 1.1 Å for α_1 and 1.0 Å for α_2. The main-chain conformation at the FG-corner is almost retained in both NiHb and deoxyHb, whereas marked changes occur at the region FG1–FG4. There is a significant movement of the FG-corner across the heme plane. Not much change is observed in the main-chain residues of the CD-region,

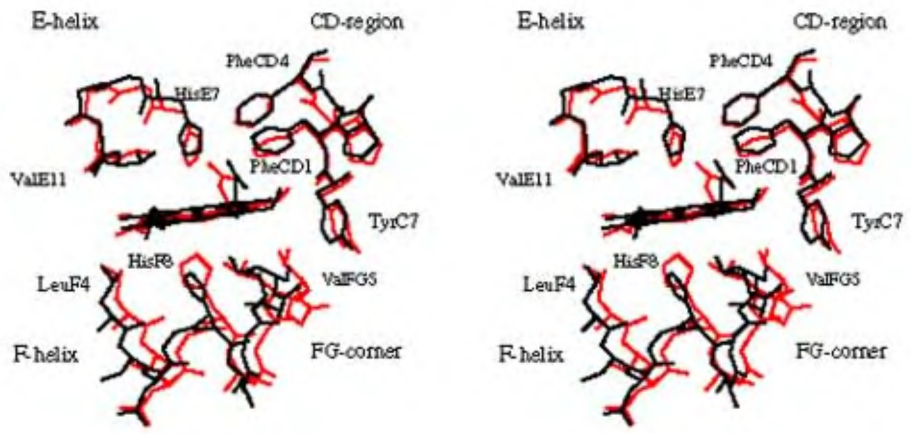

Figure 1 *a*. Stereo figure of α_1 heme pocket of deoxy T-state Hb (grey lines) and NiHb (dark lines). Structures were superimposed by least squares fitting of atoms of the heme group. Movement of the E- and F-helices away from the heme is evident.

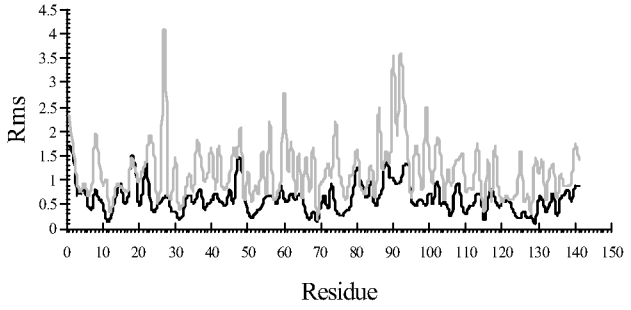

Figure 1 *b*. Residue vs rms for the superposition of α_1 chains of NiHb over deoxyHb molecule (black and gray lines show the superposition of main chain and side chain respectively).

while the side chains of PheCD4, PheCD1 and TyrC7 undergo slight changes in conformation to adapt their positions with respect to the movement of the E and F helices. The C-terminal residues Tyr140 (HC2) and Arg141 (HC3) have significant electron density and hence they are localized as in the case of deoxyHb. Thus the changes associated with α_1 and α_2 are almost the same.

Tertiary structural changes in the β-subunit

The rms deviation of the main-chain atoms at the BGH frame of reference for both β_1 and β_2 is 0.6 Å. Superposition of the heme frames in the β_1 subunit indicates a shift in the E-helix in a direction parallel to the helical axis. The F-helix has moved in a direction perpendicular to the helical axis, away from the heme plane. At β_2, the shift of the E-helix is significant and continues till the beginning of the F-helix. Unlike in β_1, the F-helix is moved slightly towards the heme pocket, whereas movement of the E-helix occurs in a direction away from the heme group as seen in Figure 2*a*. The rms difference of the main-chain atoms at the FG-corner is relatively much lower (0.4 Å in both β_1 and β_2 subunits) when compared to the α-subunits. Also, the main-chain conformation is the same at the FG-corner, except that the FG-corner is moved as a whole and this movement is propagated towards the beginning of the G-helix.

The sulphydryl group of the β93 cysteine residue in both the β-subunits, which is adjacent to the proximal histidine, retains its conformation similar to that of deoxyHb and varies with that of carbonmonoxyHb (Figure 3). The position of the C-terminal (β146) histidine is such that the side chain makes a salt bridge with the Asp (FG1) 94 which is known to be a prominent interaction for a T-state conformation. Here again, we observe that the C-terminal residues which are β145 tyrosine and β146 histidine have significant electron density in β_1 compared to β_2 (Figure 4) and are localized, thereby shielding the sulphydryl pocket of the cysteine residue.

Heme environment

It is clear from the Ni–N(ε) distances (Table 3) that at both the α-subunits, the M–N(ε) bond is broken thereby stabilizing a stable four-coordinated Ni-heme. In case of β_1, though the Ni-heme is again four-coordinated, Ni–N(ε) distance is considerably shortened compared to those in the α-subunits, whereas in case of β_2, the Ni–N(ε) distance is relatively much less compared to the α-subunits, thereby indicating a fifth coordination of proximal histidine with the metal centre. Inspection of the $2F_o–F_c$ density map clearly shows the Ni-heme electron density being pulled towards the proximal histidine (F8) (Figure 5). This closeness of density at β_2 reveals the fact that the β_2-subunit tends to prefer a five-coordinated geometry.

The heme plane in both the α-subunits as well as in β_1 are parallel to the F-helical axis, and is well shifted towards the heme pocket with respect to the F-helix frame.

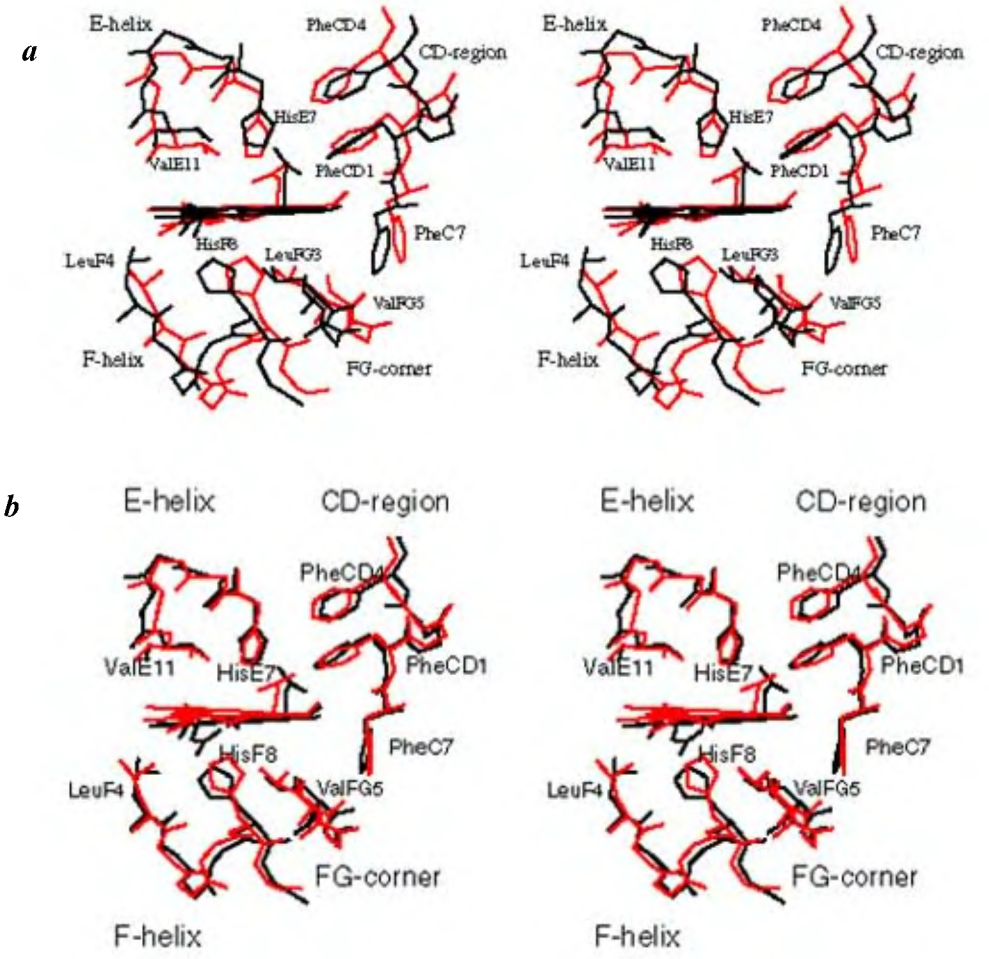

Figure 2. Stereo figure of the β_2 heme pocket of deoxy T-state Hb (grey lines) and NiHb (dark lines). ***a***, Structures were superimposed by least squares fitting of atoms of the heme moiety. Marked movement of the F-helix is evident in NiHb; ***b***, Structures were superimposed by least squares fitting of main-chain atoms of F4–F8. Movement and tilt of heme towards the F-helix is evident.

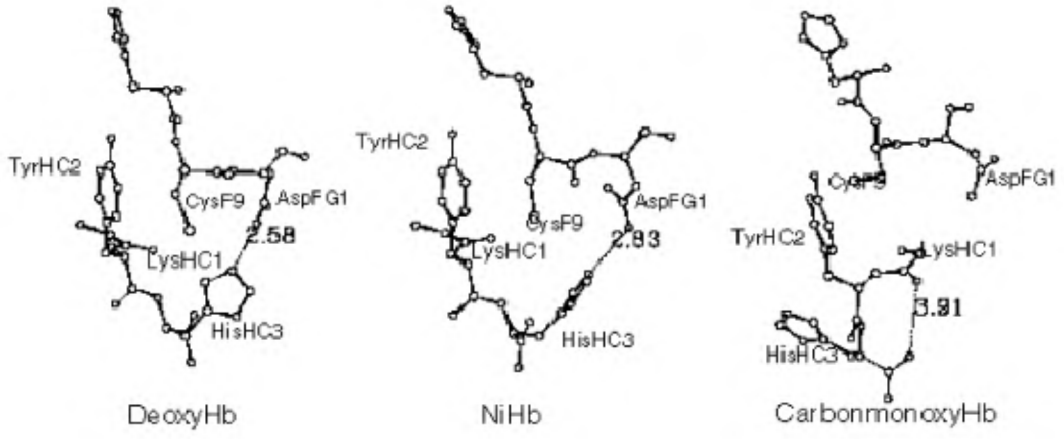

Figure 3. Sulphydryl pocket at β_2-subunit of deoxyHb, NiHb and carbonmonoxyHb.

At the β_2 subunit, the heme group still retains to be parallel to the F-helix, but with a simultaneous tilt of the plane of porphyrin, thereby facilitating a coordination with the metal centre (Figure 2 *b*).

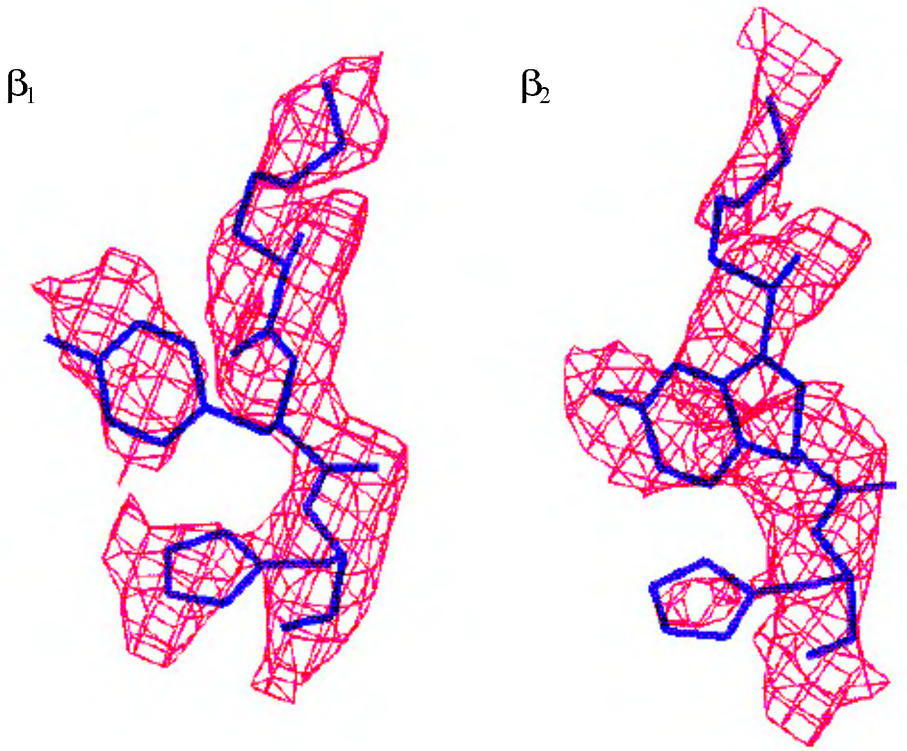

Figure 4. $2F_o$–F_c electron density map at the C-terminal regions of β_1 and β_2-subunits. Insufficient electron density at the His146 (HC3) at β_2 compared to β_1 is clearly consistent with the two different sulphydryl pockets arising from difference in the metal ion environment between the two β-subunits.

Table 2. Final refinement parameters

Resolution range (Å)	:	8.0–2.5
R-factor	:	0.242
R-free	:	0.324
Water molecules	:	38
Ramachandran outliers	:	None
Rms deviation from ideal geometry		
Bond length (Å)	:	0.017
Bond angle (°)	:	2.241
Torsion angle (°)	:	27.059
Improper angle (°)	:	1.627

Quaternary structural changes

Table 4 shows the various subunit interactions which stabilize a deoxy T-state conformation. The interface between $\alpha_1\beta_1$ and $\alpha_2\beta_2$ is formed by contacts between α_1 and β_2, and the dyad-related contacts between α_2 and β_1. The side chains of His$\beta_2$97 (FG4) packs between Thr$\alpha_1$41 (C6) and Pro$\alpha_1$44 (CD2) (Figure 6). The side chain of Aspβ_2 (G1) forms a hydrogen bond to O(ε) of Tyr$\alpha_1$42 (C7), which is similar to that of deoxyHb. The N(δ) of Asn$\alpha_1$97 (G4) forms a hydrogen bond with O(δ) of Asp$\beta_2$99 (G1). The amino group of Arg$\alpha_1$92 is in contact with the carbonyl oxygen of Pro$\beta_2$36 and the O(δ_1)94 Asp of α_1-subunit is in contact with O(δ_2) of Asp$\beta_1$99 (G1). The carbonyl group of Arg$\alpha_1$141 is salt-bridged to the amino group at the opposite α-chain, i.e. Lys$\alpha_2$127, which is similar to the one observed in deoxyHb.

Discussion

Evidence for mixed metal ion coordination

It is well known that NiHb possesses a mixture of both four- and five-coordinated forms[18,19,21–23]. This interesting feature of two different metal ion sites is strongly modulated by the protein structure, which encapsulates the heme core. The present finding indicates that the structural changes at the α-subunit are larger in magnitude than those at the β-subunits. These changes occur mainly at the FG-corner, E- and F-helices. It is clear from Figure 1 that Ni (II), being a low-spin d^8 ion, tends to favour a four-coordinated geometry without any axial ligand. This has induced a shift in E- and F-helices to move away from the heme in the α-subunits, thereby facilitating the molecule to retain a deoxy conformation. An interesting feature emerges when we compare the metal ion coordination in the hemes of NiHb with those of $\alpha_2(FeO_2)\beta_2$(Ni)[13] and α_2(Ni)β_2(FeCO)Hb[14]. While the latter two species tend towards the R-state, the former is rigorously in the T-state. In $\alpha_2(FeO_2)\beta_2$(Ni), both the β-hemes are

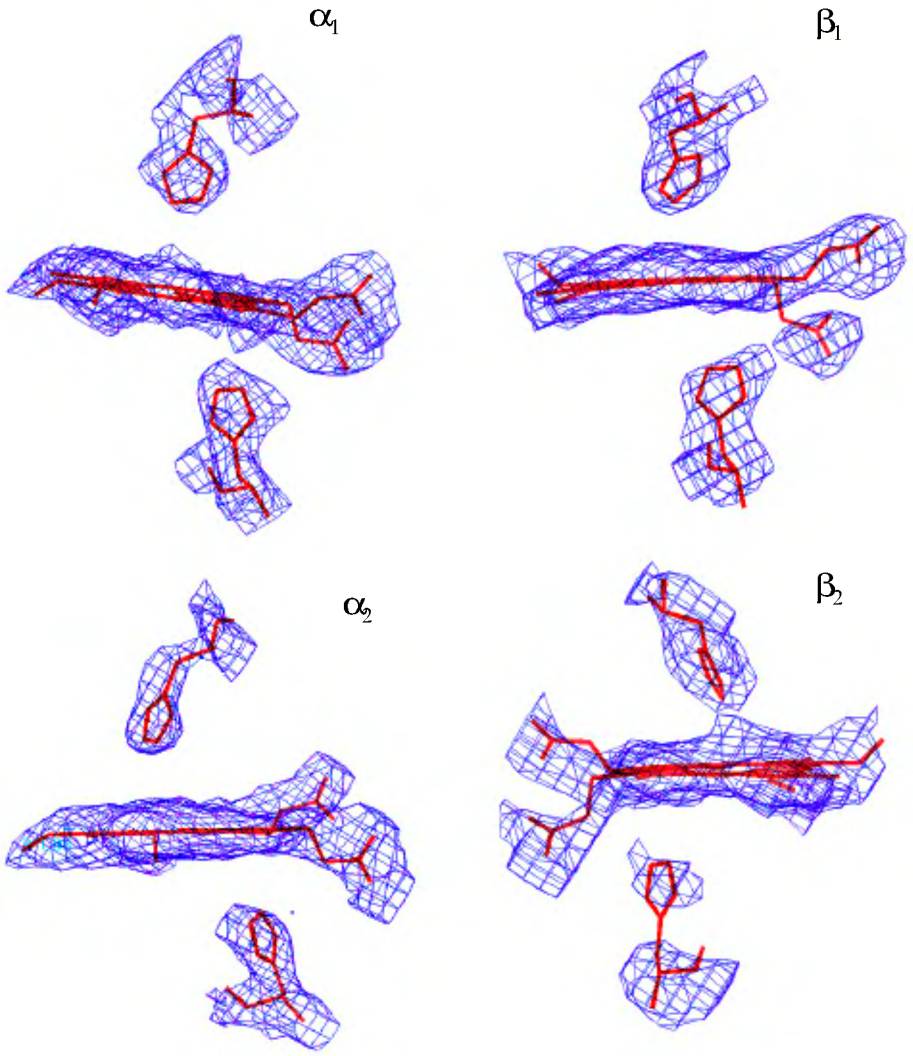

Figure 5. $2F_o$–F_c density map sectioned into the heme for clarity, with the proximal and distal histidines. The map is contoured at 1σ. With exception at the β_2 heme, the ligand and heme density is clearly consistent with a fully four-coordinated Ni metal.

Table 3. Distance of the proximal and distal histidines to the metal

Subunit	Ni–N(ε) proximal histidine (Å)	Ni–N(ε) distal histidine (Å)
α_1	3.90	4.52
α_2	4.10	4.91
β_1	3.26	4.24
β_2	3.07	4.40

penta-coordinated, as proven by both crystallography[13] and spectroscopy[22]. However, in the case of α_2(Ni)β_2 (FeCO), the Ni–N(ε) bond is broken despite the fact that this hybrid tends towards the *R*-state. Hence it is not surprising that NiHb, an example of extreme T-state as proven by spectroscopy and chemical studies (e.g. PDS reactivity profile[19]), has purely four-coordinated α-hemes and a partially five-coordinated β-heme. This indicates that R → T conformational change in these three proteins not only breaks the Ni–N(ε) bond in the α-subunit, but also weakens the same in the β-subunit.

Comparison with other spectroscopic results

Optical and chemical studies[23] show the subunits in NiHb to be in the deoxy or T-structure. UV–visible[18,19] absorption spectra revealed a split soret band characteristic of two different metal ion environments in NiHb. Later in 1986, Shelnutt *et al.*[21] investigated the state of coordination of Ni (II) in NiHb, NiMb and a variety of model Ni porphyrins (NiPPs). The Raman results are consistent with two metal ion sites as also proposed for CuHb[18], one being a four-coordinate form and the other being a five-coordinate form. Further evidence for a five-coordinate

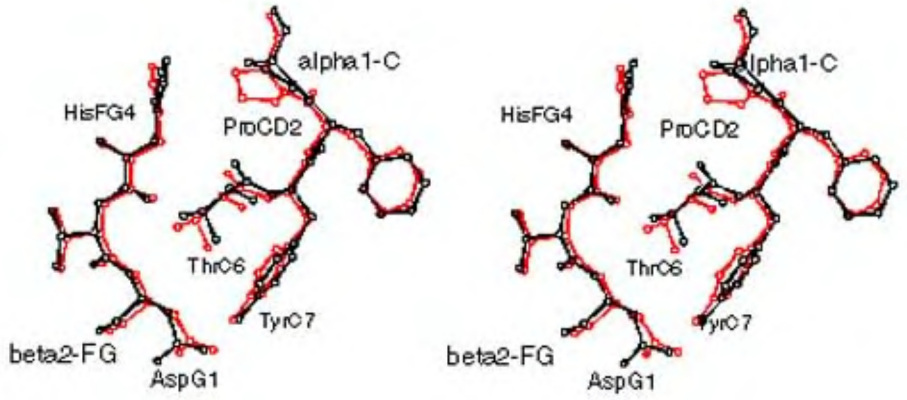

Figure 6. Stereoscopic view of α_1–β_2 interface: Packing of C-helix of α_1 and FG-corner of β_2 is shown in dark lines for NiHb and in grey lines for deoxyHb.

Table 4. Interaction between subunits at interfacial regions

α_1-subunit		β_2-subunit		Distance (Å)	
Residue	Atom	Residue	Atom	NiHb	DeoxyHb
Lys 40	C5(N^{ζ})	His 146	HC3(O^{ε})	3.81	3.16
Tyr 42	C7(OH)	Asp 99	G1(O^{δ})	2.61	2.49
Asp 94	G1(O^{δ})	Trp 37	C7(N^{ε})	3.85	2.84
Asn 97	G4(N^{δ})	Asp 99	G1(O^{δ})	3.28	2.99
Arg 141	HC3(N^{η})	Val 34	B16(O)	4.6	2.86
I. Stabilizing interactions within subunits					
Tyr 145βOH ... OC Val 98β				2.22	2.56
His 146 β Im^{+}...$^{-}$OOC Asp 94β				2.88	2.58
II. Stabilizing interactions between subunits					
Lys 127$\alpha_1$$N^{\zeta}$... OC Arg 141$\alpha_2$				2.95	2.74
Asp 126$\alpha_1$$COO^{-}$ ... $^{+}$Gua Arg 141α_2				3.35	3.01
Tyr 42α_1OH ... $^{-}$OOC Asp 99β_2				2.61	2.49

Ni(II) comes from proton nuclear magnetic resonance studies[22] of Ni-reconstituted heme proteins. The presence or absence of hyperfine-shifted proximal histydyl $N_{\delta}H$ exchangeable proton resonances provides information on the coordination and spin states of NiPP in each subunit. The hyperfine-shifted resonances at about 70.5 ppm were observed for NiHb and $\alpha_1(Fe)_2\beta_1(Ni)_2$ but not for $\alpha_1(Ni)_2\beta_1(Fe)_2$. Shibayama *et al.*[22] suggested that this could arise only when the Ni (II) assumes a high-spin ($S = 1$), five-coordinated form which is due to the proximal histidine serving as an axial ligand. Observation of temperature-dependent, broad, non-exchangeable, hydrogen-bonded proton resonances (12.6 and 10.9 ppm) and ring current-shifted broad resonances around -2 ppm in NiHb and $\alpha_2(Fe–CO)\beta_2(Ni)$ alone further substantiates the fact that NiPP is paramagnetic and five-coordinated in the β-subunit. It is significant to note that such a paramagnetic shift is not seen for the α-subunit ($\alpha_2(Ni)\beta_2(Fe)$), indicating its $S = 0$ state due to the detachment of Ni–N(ε) bond. EPR studies on spin-labelled NiHb[19] revealed two different spin-label environments as a result of different protein conformations in the same molecule.

In agreement with the aforesaid spectroscopic conclusions, our crystallographic findings reveal that the β_2-subunit tends to be five-coordinated, while both the α-subunits and the β_1-subunit remain four-coordinated in the most T-structured NiHb. This is clear from a closer inspection of the $2F_o–F_c$ electron density of the heme region in all four subunits (Figure 5). Movement of the F-helix is such that there is a simultaneous tilt and displacement of the imidazole ring towards the heme pocket (Figure 2*a*). Although the Ni–N(ε) proximal histidine distance seems to be slightly higher than that of a bonding distance (Table 3), closeness of the electron density of histidine near the heme is indicative of a preferential five-coordination of the Ni (II) in β_2. Similarly, the elec-

tron density of histidine in β_1 is far closer to those in the α-subunit, though a little far-off compared to the β_2-subunit. It is important to point out that Shelnutt *et al.*[21] observed (i) a low value for Ni–N(ε) stretching frequency at 236 cm^{-1} in NiHb, indicating a weak five-coordination, and (ii) only a decrease of almost 7 cm^{-1} in the Ni–ligand stretch in NiHb, upon ^{64}Ni-isotopic substitution, against a prediction of 10 cm^{-1} for a pure Ni–ligand stretch as in the case for NiMb. Thus, our studies strongly suggest that the weak five-coordination is reflected more in the β_2 than in the β_1-subunit, which is again reflected in the C-terminal regions (Figure 4).

However, at a resolution of 2.5 Å, an error of 0.2 Å is most likely in atomic coordinates; this would mean that Ni–N(ε) (proximal) bonds can be 3.1–3.3 Å in both the β-subunits, prompting us to suggest equivalence of β_1 and β_2-subunits in the heme area, with a five-coordinate being described as four from basal porphyrin and a weak interaction with a more distant proximal histidine. A comment is needed on this fifth weak coordination at a distance of ~3.1 Å. Such a kind of long-distance coordination (~3.0 Å) has been substantiated earlier by Solomon and coworkers[29] in the case of blue copper proteins.

Structural changes at the α_1–β_2 interface

Baldwin and Chothia[27] have explored in detail the quaternary changes associated with tertiary structural changes during T ↔ R transition. The α_1–β_1 dimer forms several contacts with the α_2–β_2 dimer, which serves as a signal-transmitting pathway between subunits on ligand binding. It is observed from our finding that the residues in contact between α_1C and β_2FG which is considered as the 'switch region' are still retained in NiHb (Figure 6), similar to that of deoxyHb. Whereas more dramatic changes occur at the α_1FG–β_2C core, which is considered as the 'Flexible region'. It has been previously noted by Max Perutz[23], on the basis of preliminary X-ray study on NiHb, that although NiHb, assumes a T-state conformation there exists certain significant structural changes with respect to deoxyHb. It is now clear from our present structural analysis on NiHb, that the significant structural changes are due to the four-coordinated Ni-heme at the α-subunit which has induced certain structural perturbations in the heme pocket, F-helix and FG-corner. It is to be noted in this context that a four-coordinated metal porphyrin, which is less constrained inside the hydrophobic globin pocket, is likely to enjoy a greater vibrational freedom. We believe from our present investigation that this small but significant delocalization of the four-coordinated Ni-heme mainly in the α-subunit has induced the proximal F8 histidine to move away from the heme moiety which has influenced the structural perturbation at the Valα93(FG5), as also observed by Ho[30] for conformational changes between T and R states. This perturbation is transmitted to Tyrα140(HC2) and then across the interface to Trpβ37(C3) and then Argβ40(C6) (by way of Thrβ38(C4) and Glnβ39(C5)), Tyrα42(C7), Aspβ99(G1) and Valβ98(FG5), and finally to the β-heme. This is illustrated in Scheme 1. Thus heme–heme interaction is likely to operate synchronously to transmit conformational changes from one subunit to the neighbouring subunit.

Role of β93 Cys

The sulphydryl group of β93 Cys residue is well documented as a reporter group for monitoring the conformational changes occurring in the molecule[31,32]. Figure 3 illustrates that in case of NiHb, the SH-group retains the same conformation as in the case of the deoxy structure. The presence of a strong hydrogen bond between the Asp FG1 and the side chain of histidine reveals the fact that the SH-group of β93 Cys is further hindered in case of a T-state molecule. This is in accordance with the previous studies on the very low reactivity of the SH-group of β93 Cys towards PDS in case of NiHb[18]. In spite of the same conformation being retained in both β_1 and β_2-subunits, the appearance of significant electron density only in the C-terminal histidine of β_1-subunit indicates the inequivalent flexibility of the terminal histidine between the two β-subunits (Figure 4). Thus, it is convincing from this study that the two slightly differing metal-ion environments of the β-subunits have in turn resulted in different sulphydryl pockets which is in exact agreement with the earlier reported EPR studies on spin-labelled NiHbs[31]. It may be noted that Manoharan and coworkers[31] observed two different immobile components, as seen from different $2T_{\|}$ values, in NiHb when the β93 SH group was attached with longer spin labels.

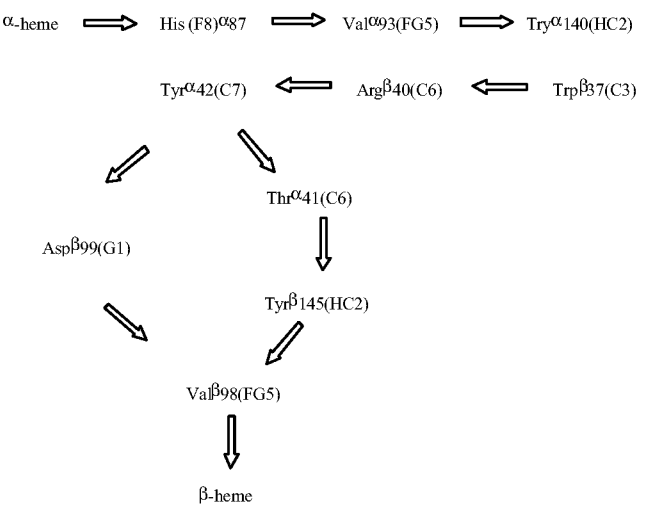

Scheme 1. Conformational changes.

Conclusion

Our present crystallographic studies on NiHb confirm that it takes up a structure similar to that of deoxyHb. The unique feature of a five-coordinated NiPP is confined to the β_2-subunit in NiHb. However, there exist certain structural changes in the F-helix to FG-corner, which lead to significant differences in the subunit contact regions. High-resolution data using synchrotron radiation could provide more insight on the nature of the planarity of porphyrin, and further details on subunit inequivalence could lead to a better understanding of the structural basis of ligand binding to tetrameric heme proteins.

1. Eaton, W. A., Henry, E. R., Hofrichter, J. and Mozzarelli, A., *Nature – Struct. Biol.*, 1999, **6**, 351–357.
2. Perutz, M. F., Wilkinson, A., Paoli, M. and Dodson, G., *Annu. Rev. Biophys. Biomol. Struct.*, 1998, **27**, 1–34.
3. Gelin, B. R., Wai-Mun lee, A. and Karplus, M., *J. Mol. Biol.*, 1983, **171**, 489–559.
4. Monod, J., Wyman, J. and Changeux, J. P., *ibid*, 1965, **12**, 88–118.
5. Pauling, L., *Proc. Natl. Acad. Sci. USA*, 1935, **21**, 186–191.
6. Koshland, D. E., Nemethy, G. and Filmer, D., *Biochemistry*, 1966, **5**, 365–385.
7. Perutz, M. F., *Nature*, 1970, **228**, 226–233.
8. Ackers, G. K., Doyle, M. L., Myers, D. M. and Daugherty, M. A., *Science*, 1992, **255**, 54–63.
9. Venkatesh, B., Manoharan, P. T. and Rifkind, J. M., *Progress in Inorganic Chemistry* (ed. Karlin, K. D.), 1997, p. 47.
10. Kuila, D., Natan, M. J., Rogers, P., Gingrich, D. J., Baxter, W. W., Arnone, A. and Hoffmann, B. M., *J. Am. Chem. Soc.*, 1991, **113**, 6520–6526.
11. Moffat, K., Loe, R. S. and Hoffman, B. M., *ibid*, 1974, **96**, 5259–5261.
12. Fermi, G. and Perutz, M. F., *J. Mol. Biol.*, 1982, **155**, 495–505.
13. Luisi, B. and Shibayama, N., *ibid*, 1989, **206**, 723–736.
14. Luisi, B., Liddington, B., Fermi, G. and Shibayama, N., *ibid*, 1990, **214**, 7–14.
15. Bruno, S. *et al.*, *Protein Sci.*, 2000, **9**, 689–692.
16. Park, S., Nakagawa, A. and Morimoto, H., *J. Mol. Biol.*, 1996, **255**, 726–734.
17. Arnone, A., Rogers, P., Blough, N., McGourty, J. and Hoffman, B., *ibid*, 1986, **188**, 693–706.
18. Manoharan, P. T., Alston, K. and Rifkind, J. M., *J. Am. Chem. Soc.*, 1986, **108**, 7095–7100.
19. Manoharan, P. T., *Proc. Indian Acad. Sci., Chem. Sci.*, 1990, **102**, 337–352.
20. Shibayama, N., Morimoto, H. and Kitagawa, T., *J. Mol. Biol.*, 1986, **192**, 331–336.
21. Shelnutt, J. A., Alston, K., Jui-YuanHo, Nai-TengYu, Yomamoto, T. and Rifkind, J. M., *Biochemistry*, 1986, **25**, 620–627.
22. Shibayama, N., Inubushi, T., Morimoto, H. and Yonetani, T., *ibid*, 1987, **26**, 2194–2201.
23. Alston, K., Schechter, A. N., Arcoleo, J. P., Greer, J., Parr, G. R. and Friedman, F. K., *Haemoglobin*, 1984, **8**, 47–60.
24. Drabkin, D. L., *J. Biol. Chem.*, 1946, **164**, 703–723.
25. Huber, R., Proceedings of the Daresbury Study Weekend, Warrington, Daresbury Laboratory, 1985, pp. 58–61.
26. Waller, D. A. and Liddington, R. C., *Acta Crystallogr. Sect. B*, 1990, **46**, 409–418.
27. Baldwin, J. and Chothia, C., *J. Mol. Biol.*, 1979, **129**, 175–220.
28. Liddington, R., Derewenda, Z., Dodson, E., Hubbard, R. and Dodson, G., *ibid*, 1992, **228**, 551–579.
29. Solomon, E. I., Uma, M. S. and Machonkin, T. E., *Chem. Rev.*, 1996, **96**, 2563–2605.
30. Ho, C., *Adv. Protein. Chem.*, 1992, **43**, 152–312.
31. Manoharan, P. T., Wang, J. T., Alston, K. and Rifkind, J. M., *Haemoglobin*, 1990, **14**, 41–67.
32. Vasquez, G. B., Karavitis, M., Ji, X., Pechik, I., Brinigar, W. S., Gilliland, G. L. and Fronticelli, C., *Biophys. J.*, 1999, **76**, 88–97.

ACKNOWLEDGEMENTS. S.V. thanks the Indian Institute of Technology – Madras for a fellowship and P.T.M. thanks CSIR, New Delhi and IIT, Madras for emeritus positions and DST, Govt. of India, New Delhi for a grant. Help from the National Facility for Macromolecular X-ray Data Collection at the Molecular Biophysics Unit, Indian Institute of Science, Bangalore is gratefully acknowledged.

Received 22 July 2002; revised accepted 18 November 2002